Neurobiology of Disease

Presenilin/γ-Secretase Activity Is Located in Acidic Compartments of Live Neurons

Masato Maesako,[1] Mei C. Q. Houser,[1] Yuliia Turchyna,[1] Michael S. Wolfe,[2] and Oksana Berezovska[1]
[1]Alzheimer Research Unit, MassGeneral Institute for Neurodegenerative Disease, Massachusetts General Hospital, Harvard Medical School, Charlestown, Massachusetts 02129, and [2]Department of Medicinal Chemistry, University of Kansas, Kansas 66045

Presenilin (PSEN)/γ-secretase is a protease complex responsible for the proteolytic processing of numerous substrates. These substrates include the amyloid precursor protein (APP), the cleavage of which by γ-secretase results in the production of β-amyloid (Aβ) peptides. However, exactly where within the neuron γ-secretase processes APP C99 to generate Aβ and APP intracellular domain (AICD) is still not fully understood. Here, we employ novel Förster resonance energy transfer (FRET)-based multiplexed imaging assays to directly "visualize" the subcellular compartment(s) in which γ-secretase primarily cleaves C99 in mouse cortex primary neurons (from both male and female embryos). Our results demonstrate that γ-secretase processes C99 mainly in LysoTracker-positive low-pH compartments. Using a new immunostaining protocol which distinguishes Aβ from C99, we also show that intracellular Aβ is significantly accumulated in the same subcellular loci. Furthermore, we found functional correlation between the endo-lysosomal pH and cellular γ-secretase activity. Taken together, our findings are consistent with Aβ being produced from C99 by γ-secretase within acidic compartments such as lysosomes and late endosomes in living neurons.

Key words: **Alzheimer's disease; FRET; intracellular Aβ; lysosomes; presenilin/γ-secretase**

Significance Statement

Alzheimer's disease (AD) genetics and histopathology highlight the importance of amyloid precursor protein (APP) processing by γ-secretase in pathogenesis. For the first time, this study has enabled us to directly "visualize" that γ-secretase processes C99 mainly in acidic compartments such as late endosomes and lysosomes in live neurons. Furthermore, we uncovered that intracellular β-amyloid (Aβ) is significantly accumulated in the same subcellular loci. Emerging evidence proposes the great importance of the endo-lysosomal pathway in mechanisms of misfolded proteins propagation (e.g., Tau, α-Syn). Therefore, the predominant processing of C99 and enrichment of Aβ in late endosomes and lysosomes may be critical events in the molecular cascade leading to AD.

Introduction

The accumulation of β-amyloid (Aβ) peptides in the brain in the form of neuritic plaques is one of the pathologic hallmarks of Alzheimer's disease (AD). The United States Food and Drug Administration has recently approved an anti-Aβ antibody for the treatment of AD (Sevigny et al., 2016). While the drug showed a dose-dependent reduction in Aβ levels in the brain, the efficacy of the drug to improve cognition remains controversial because of conflicting clinical data. Aβ is generated from the sequential processing of the amyloid precursor protein (APP). First, β-secretase processes APP, resulting in shedding of the APP ectodomain and generation of the 99-residue APP C-terminal fragment β (C99; Vassar et al., 1999). C99 is subsequently processed by γ-secretase (De Strooper et al., 1998; Wolfe et al., 1999), producing various lengths of Aβ peptides, including the membrane-anchored longer Aβ (Aβ45–49) and shorter Aβ (Aβ38–43) that are released from the membrane (Funamoto et al., 2004; Qi-Takahara et al., 2005; Takami et al., 2009). Presenilin (PSEN) functions as the catalytic subunit of γ-secretase (Wolfe et al., 1999) and two homologous PSEN proteins exist: PSEN1 and PSEN2 (Levy-Lahad et al., 1995; Sherrington et al., 1995). Numerous dominant mutations that result in early-onset familial AD (FAD) have been identified on the genes encoding APP, PSEN1 and PSEN2 (https://www.alzforum.org/mutations), suggesting that C99 (Lauritzen et al., 2019), Aβ

Received Aug. 20, 2021; revised Oct. 21, 2021; accepted Nov. 15, 2021.

Author contributions: M.M., M.S.W., and O.B. designed research; M.M., M.C.Q.H., and Y.T. performed research; M.C.Q.H. and Y.T. contributed unpublished reagents/analytic tools; M.M., M.C.Q.H., and Y.T. analyzed data; M.M. wrote the first draft of the paper; M.M., M.C.Q.H., M.S.W., and O.B. edited the paper; M.M. and O.B. wrote the paper.

This work was supported by the BrightFocus Foundation Grant A2019056F (to M.M.) and National Institutes of Health Grants AG 44486 (to O.B.) and AG 15379 (to O.B.). We thank Dr. Steven S Hou (Massachusetts General Hospital Neurology) for kind support on data analysis and helpful discussion and Mr. Alec K. McKendell (Massachusetts General Hospital Neurology) for helping with data analysis.

The authors declare no competing financial interests.

Correspondence should be addressed to Masato Maesako at mmaesako@mgh.harvard.edu.

https://doi.org/10.1523/JNEUROSCI.1698-21.2021

(Selkoe and Hardy, 2016), and/or APP intracellular domain (AICD; Pardossi-Piquard and Checler, 2012) are mechanistically involved in the pathogenesis of FAD.

One of the important questions that remains unclear is which subcellular compartment(s) γ-secretase processes C99 and generates Aβ peptides and AICD in neurons. While APP and PSEN1 are mainly co-localized in the Golgi and ER (Cupers et al., 2001; Berezovska et al., 2003), Förster resonance energy transfer (FRET) and fluorescence lifetime imaging microscopy (FLIM) enabled us to elucidate that APP and PSEN1 come into closest proximity primarily in compartments near the cell surface (Berezovska et al., 2003). A recent study employing super-resolution microscopy also highlighted the association of PSEN1 with APP at the cell surface (Escamilla-Ayala et al., 2020). However, not all of the expressed γ-secretase complexes seem to be functionally active (Lai et al., 2003; Placanica et al., 2009), and therefore the APP-PSEN proximity may not directly indicate where the protease cleaves the substrate. Earlier studies proposed that γ-secretase cleaves C99 and generates Aβ rather in the endo-lysosomal pathway. For example, cell surface APP labeled by radioisotope or antibody is endocytosed and processed into Aβ, which is released into an extracellular region or retained in the cells (Haass et al., 1992; Koo and Squazzo, 1994; Koo et al., 1996). Aβ secreted from cultured cells is significantly reduced by the treatment of drugs that prevent endo-lysosomal acidification, such as ammonium chloride (Schrader-Fischer and Paganetti, 1996). Electron microscopy and biochemical analysis demonstrated the enrichment of Nicastrin expression, a subunit of γ-secretase, and increased γ-secretase activity in lysosomes (Pasternak et al., 2003). Recently, it was also illustrated that while PSEN1 is broadly distributed in the cell, PSEN2 is predominantly localized in late endosomes and lysosomes (Meckler and Checler, 2016; Sannerud et al., 2016; Watanabe et al., 2021), where it is responsible for the generation of an intracellular pool of Aβ (Sannerud et al., 2016). Importantly, FAD-causing PSEN2 mutations promote the production of intracellular Aβ (Aβ42 in particular) and several PSEN1 FAD mutants phenocopy FAD PSEN2 with respect to of subcellular localization and intracellular Aβ42 generation (Sannerud et al., 2016).

Here, we aim to directly visualize the subcellular compartment(s) in which γ-secretase primarily cleaves APP C99 and where intracellular Aβ resides in intact/live neurons. For such, we developed new multiplexed imaging assays employing our recently engineered C99 720–670 FRET biosensor (Houser et al., 2020). The cleavage of the C99 720-670 biosensor by endogenous γ-secretase results in decreased FRET between miRFP670 (donor) and miRFP720 (acceptor), and thus the measurement of acceptor over donor ratio permits quantitative monitoring of γ-secretase activity in live cells. More importantly, miRFP670 and miRFP720 are the most red-shifted, fully near-infrared (NIR) FRET pair, being compatible with reporter probes and/or fluorescent dyes in the visible spectrum range (Shcherbakova et al., 2016, 2018). This unique spectral property has enabled for the first time recording of γ-secretase activity along with other biological events in individual cells (Houser et al., 2020). Using the multiplexing capability, we uncovered the LysoTracker-positive acidic compartments as a primary site where endogenous γ-secretase processes the C99 720-670 biosensor in primary neurons. Time-lapse imaging of live neurons revealed the dynamic and heterogeneous nature of the C99 720-670 biosensor processing. Furthermore, we developed a new antibody-based imaging platform to visualize intracellular Aβ, and found that Aβ is significantly concentrated in the same subcellular loci where γ-secretase primarily processes the C99 720-670 biosensor. Lastly, the cell-by-cell based multiplexed imaging illustrated abnormally high endo-lysosomal pH in the neurons with diminished endogenous γ-secretase activity. Emerging evidence proposes the great importance of endo-lysosomal membrane integrity in mechanisms of cellular invasion by misfolded proteins (e.g., Tau, α-Syn; Polanco et al., 2021; Polanco and Götz, 2021). Therefore, the enrichment of intracellular Aβ in the same acidic compartments may be one of the critical events in the molecular cascade leading to AD.

Materials and Methods

Plasmid DNA and adeno-associated virus (AAV) development

The cDNA of C99 720-670 biosensor (Houser et al., 2020) was subcloned into a pAAV2/8 vector containing human Synapsin 1 promoter (Maesako et al., 2017, 2020). The sequence of plasmid used in this study was verified by MGH CCIB DNA core. The packaging into AAV was performed by University of Pennsylvania Gene Therapy Program vector core (Philadelphia, PA; 2.56 E + 13 GC/ml).

Primary neuronal culture

Primary neurons were obtained from cerebral cortex of from both male and female mouse embryos at gestation days 14–16 (Charles River Laboratories). Papain Dissociation System (Worthington Biochemical Corporation) was used to dissociate neurons, which were maintained for 13–15 d *in vitro* (DIV) in Neurobasal medium containing 2% B27 supplement, 1% GlutaMAX Supplement, and 1% penicillin streptomycin (Pen Strep; Thermo Fisher Scientific). The neuronal preparation procedure was approved by the Massachusetts General Hospital Animal Care and Use Committee (protocol #2003N000243).

Immunocytochemistry

Primary neurons were fixed with 4% paraformaldehyde (PFA; VWR), and permeabilized by 0.1% Triton X-100. The permeabilized neurons were incubated with primary antibodies, followed by an Alexa Fluor 488 or Cy3-conjugated secondary antibodies (Thermo Fisher Scientific). The slide was covered by a coverslip (Fisher Scientific) using Fluoromount-G Mounting Medium (Thermo Fisher Scientific). An anti-Aβ (6E10) antibody was purchased from BioLegend, anti-LAMP1 antibody was from MilliporeSigma, and anti-Rab7 and anti-Rab5 antibodies were from Cell Signaling Technology. To stain acidic compartments in live neurons, LysoTracker Green DND-26, LysoSensor Yellow/Blue DND-160 and pHrodo Green Dextran, 10,000 MW (Thermo Fisher Scientific) were used according to the manufacture's protocol. γ-Secretase inhibitor: DAPT and vehicle DMSO were purchased from Sigma-Aldrich.

Confocal microscopy

The diode laser at wavelengths of 405 nm (LysoSensor Yellow/Blue DND-160), 488 nm (LysoTracker Green DND-26, pHrodo Green Dextran, and Alexa Fluor 488) and 640 nm (miRFP670 in the C99 720-670 biosensor) was used for excitation. The emitted fluorescence was detected at 500–530 nm (LysoTracker Green DND-26, pHrodo Green Dextran, and Alexa Fluor 488), at 430–470 nm and 530–570 nm (LysoSensor Yellow/Blue DND-160), at 570-620 nm (Cy3), and at 660-680 nm (miRFP670) and 700–720 nm (miRFP720; C99 720-670 biosensor) using the Standard and High-sensitive detectors on an Olympus FV3000RS Confocal Laster Scanning Microscope. A CO_2/heating unit (Tokai-Hit STX-Co2 Digital CO_2 Gas Mixing System, STFX model) was used to maintain suitable CO_2 concentration and heating for live neurons. 10×/0.25 NA and 60×/1.30 NA objectives were used for imaging. Pseudo-colored images corresponding to the emission intensity of miRFP720 over miRFP670 (γ-secretase activity) and 6E10 over miRFP720 (intracellular Aβ) ratios were generated in MATLAB (The MathWorks).

ELISA

The conditioned medium of primary neurons expressing the C99 720-670 biosensor was used to measure human Aβ40 and Aβ42 levels. The

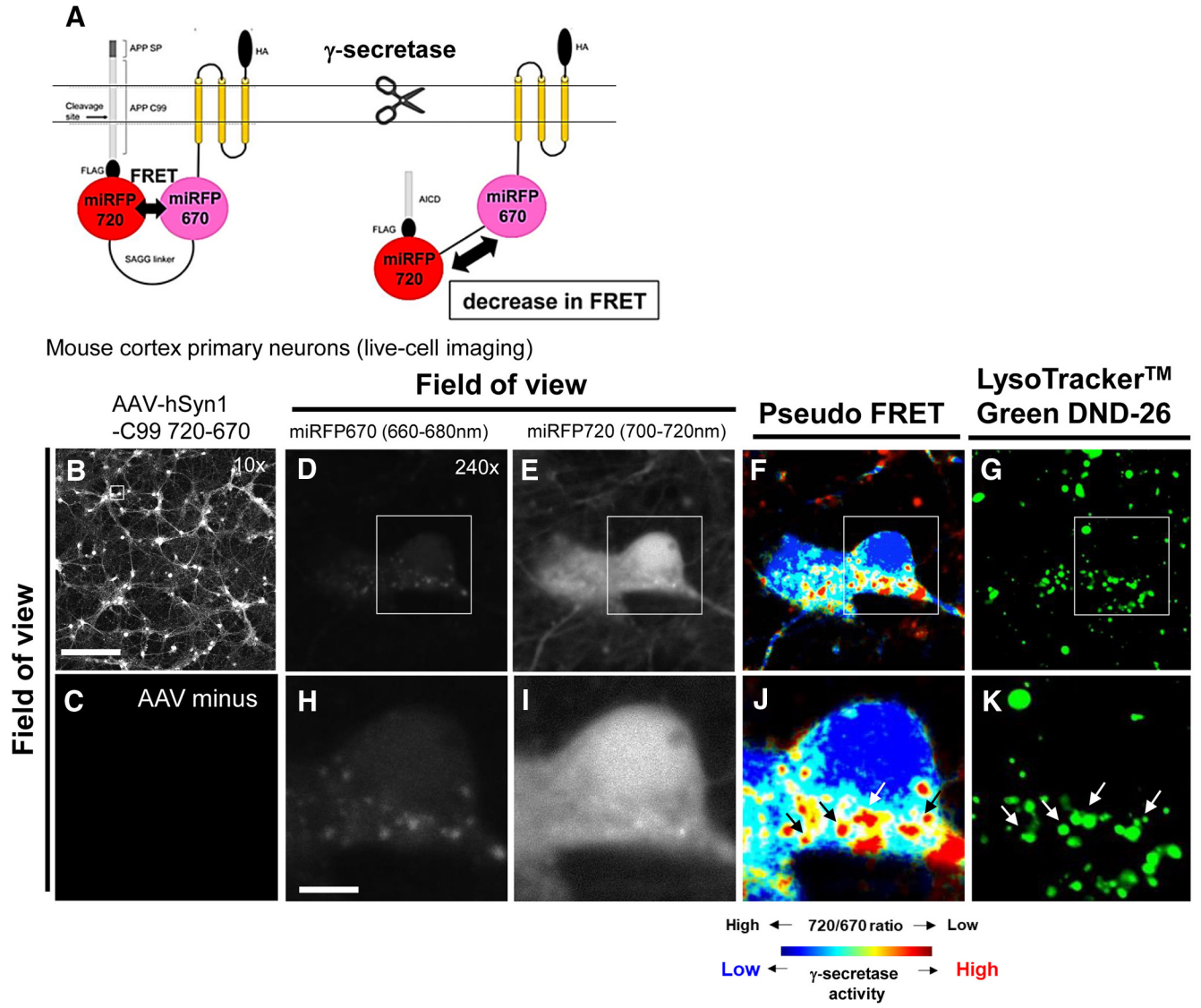

Figure 1. The C99 720-670 biosensor processing by γ-secretase in acidic compartments of neurons. ***A***, A schematic presentation of the C99 720-670 biosensor. Low-magnification (10×) images of neurons transduced with an AAV-hSyn1-C99 720-670 (***B***) compared with the neurons without AAV transduction (***C***) indicate successful expression of the C99 720-670 biosensor. Scale bar: 250 µm. High-magnification images of neurons display miRFP670 emission (***D***), miRFP720 emission (***E***), pseudo-colored miRFP720 over 670 emission ratios (pseudo FRET; i.e., lower ratio = more processing by γ-secretase: highlighted by red; ***F***), and LysoTracker Green DND-26 emission (***G***). Scale bar: 10 µm (***H–K***). Higher magnification images corresponding to the squared area in ***D–G***.

Human Amyloid (1–40) ELISA kit Wako II and Human Amyloid (1–42) ELISA kit Wako were used according to the manufacture's protocol (FUJIFILM Wako Pure Chemical Corporation).

Statistics

GraphPad Prism 9 (GraphPad Software) was used to perform statistical analysis. The D'Agostino and Pearson omnibus normality test was applied to examine the Gaussian distribution of the data and the variance equality. Unpaired Student's *t* test or Mann–Whitney *U* test was applied to compare the data. The Pearson correlation coefficient was applied to measure linear correlation; $p < 0.05$ was considered a predetermined threshold for statistical significance and all values are given as means ± SD.

Results

γ-Secretase primarily processes APP C99 in acidic compartments of neurons

While FRET/FLIM and super-resolution microscopy revealed closer proximity between APP and PSEN1 near and/or at the cell surface (Berezovska et al., 2003; Escamilla-Ayala et al., 2020), earlier biochemical studies suggested that Aβ is generated rather in the endo-lysosomal compartments (Haass et al., 1992; Koo and Squazzo, 1994; Schrader-Fischer and Paganetti, 1996; Koo et al., 1996; Pasternak et al., 2003). Recent studies shed light on the restricted localization of PSEN2 in late endosomes and lysosomes (Meckler and Checler, 2016; Sannerud et al., 2016; Watanabe et al., 2021), and the role of PSEN2/γ-secretase in the generation of intracellular Aβ (Sannerud et al., 2016). To directly visualize where γ-secretase processes C99 and thus generates Aβ peptides, we employed high-resolution confocal microscopy and our recently developed C99 720-670 biosensor (Houser et al., 2020). We have previously validated that our FRET biosensors are integrated into the membrane, trafficked through the secretory pathway, and as efficiently processed by endogenous γ-secretase as C99-FLAG is. Moreover, this processing leads to changes in the orientation and/or proximity between miRFP670

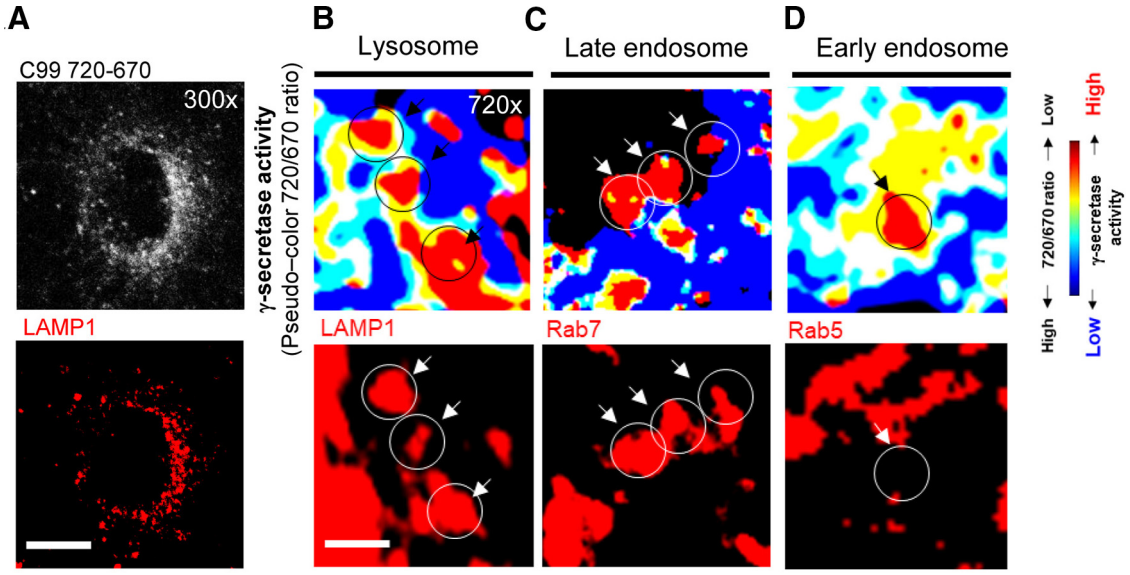

Figure 2. Colocalization analysis of the C99 720-670 cleavage and endo-lysosomal markers. ***A***, A representative low-magnification image of the neurons expressing the C99 720-670 biosensor stained with an anti-LAMP1 antibody. Scale bar: 10 μm. ***B***, Higher magnification pseudo-colored images corresponding the 720/670 ratios (i.e., lower ratio = more γ-secretase activity: highlighted by red; top panels) and LAMP1 (a lysosome marker), (***C***) Rab7 (late endosome), or (***D***) Rab5 (early endosome), indicating colocalization of the C99 720-670 cleaving sites with late endosomes and lysosomes. Scale bar: 2 μm.

(donor) and miRFP720 (acceptor) fluorophores. This results in decreased FRET between donor and acceptor, and thus the measurement of 720 over 670 emission ratio permits quantitative monitoring of γ-secretase activity in live cells (i.e., a decreased 720/670 ratio indicates increased γ-secretase activity; Houser et al., 2020; Maesako et al., 2020; Fig. 1*A*).

Mouse cortex primary neurons were transduced with an AAV packaging the C99 720-670 biosensor. Low-magnification (10×) images show successful expression of the C99 720-670 biosensor in neurons (Fig. 1*B*,*C*). Then we acquired high-magnification images (240×) to identify in which subcellular compartments γ-secretase is functional. We found significantly lower 720/670 ratios in the vesicle-shaped areas (Fig. 1*D*–*F*,*H*–*J*), suggesting that γ-secretase primarily cleaves the C99 720-670 biosensor in these particular cytoplasmic compartments of the neuron. To characterize the vesicle-shaped compartments displaying the predominant processing of the C99 720-670 probe, we incubated the neurons with LysoTracker Green DND-26 which stains acidic compartments (e.g., late endosomes, lysosomes). Strikingly, we found that the compartments showing lower 720/670 ratios co-localized with LysoTracker Green fluorescence signals (Fig. 1*F*,*G*,*J*,*K*), demonstrating that γ-secretase mainly cleaves the C99 720-670 biosensor in acidic compartments.

To further ensure that γ-secretase processes the C99 720-670 biosensor in late endosomes and lysosomes, neurons expressing the C99 720-670 biosensor were fixed and stained with the antibodies against endo-lysosomal markers (Fig. 2*A*, representative whole-cell image with LAMP1). We found that the subcellular areas with decreased 720/670 ratios (i.e., C99 cleavage by γ-secretase) are positive with LAMP1 (lysosomes; Fig. 2*B*) or Rab7 (late endosomes; Fig. 2*C*). On the other hand, the area with lower 720/670 ratios rarely overlapped with Rab5 (early endosomes; Fig. 2*D*). Altogether, these results suggest that γ-secretase predominantly processes the C99 720-670 biosensor in late endosomes and lysosomes within the neuron.

Spatiotemporally dynamic and heterogeneous processing of APP C99 in neurons

Next, we performed time-lapse FRET imaging in live cells to better understand the spatiotemporal regulation of C99 processing by γ-secretase with subcellular resolution. In this experiment, the emission of donor and acceptor in primary neurons expressing the C99 720-670 biosensor were simultaneously detected every 10 min for 30 min. First, we found that γ-secretase "dynamically" processes C99 in the same compartments within the 30-min imaging period (Fig. 3*A*–*D*). For example, 720/670 ratios were higher at 10 and 20 min compared with that of baseline in the region of interest (ROI)#1 (Fig. 3*D*,*E*). We assume this increase in the ratio might be because the newly synthesized C99 720-670 biosensor was delivered to the ROI within the 10 min between baseline and 10-min imaging point, increasing an averaged 720/670 ratio in the ROI. However, we found a significantly lower 720/670 ratio at 30 min than 20 min time point (Fig. 3*D*, *E*), suggesting that γ-secretase actively processed the C99 720-670 biosensor within the last 10 min. A similar processing pattern was observed in ROI#2 (Fig. 3*D*,*E*), demonstrating that γ-secretase processes C99 in a temporally dynamic manner.

On the other hand, we found that ROI#3 showed consistently lower 720/670 ratios from baseline to 20 min time point compared with that at 30 min recording (Fig. 3*D*,*E*). Furthermore, ROI#4 displayed high 720/670 ratios, which were not changed during the entire imaging period (Fig. 3*D*,*E*). These results suggest that when γ-secretase cleaves C99 varies among compartments. Altogether, the time-lapse FRET imaging demonstrates the spatiotemporally dynamic but heterogeneous nature of C99 processing by γ-secretase within the neuron.

Aβ accumulation in the compartments with predominant C99 processing by γ-secretase

To further validate the enrichment of γ-secretase activity in late endosomes and lysosomes, neurons expressing the C99 720-670 biosensor were stained with anti-Aβ (6E10) and Alexa Fluor 488-conjugated secondary antibodies. The 6E10 antibody

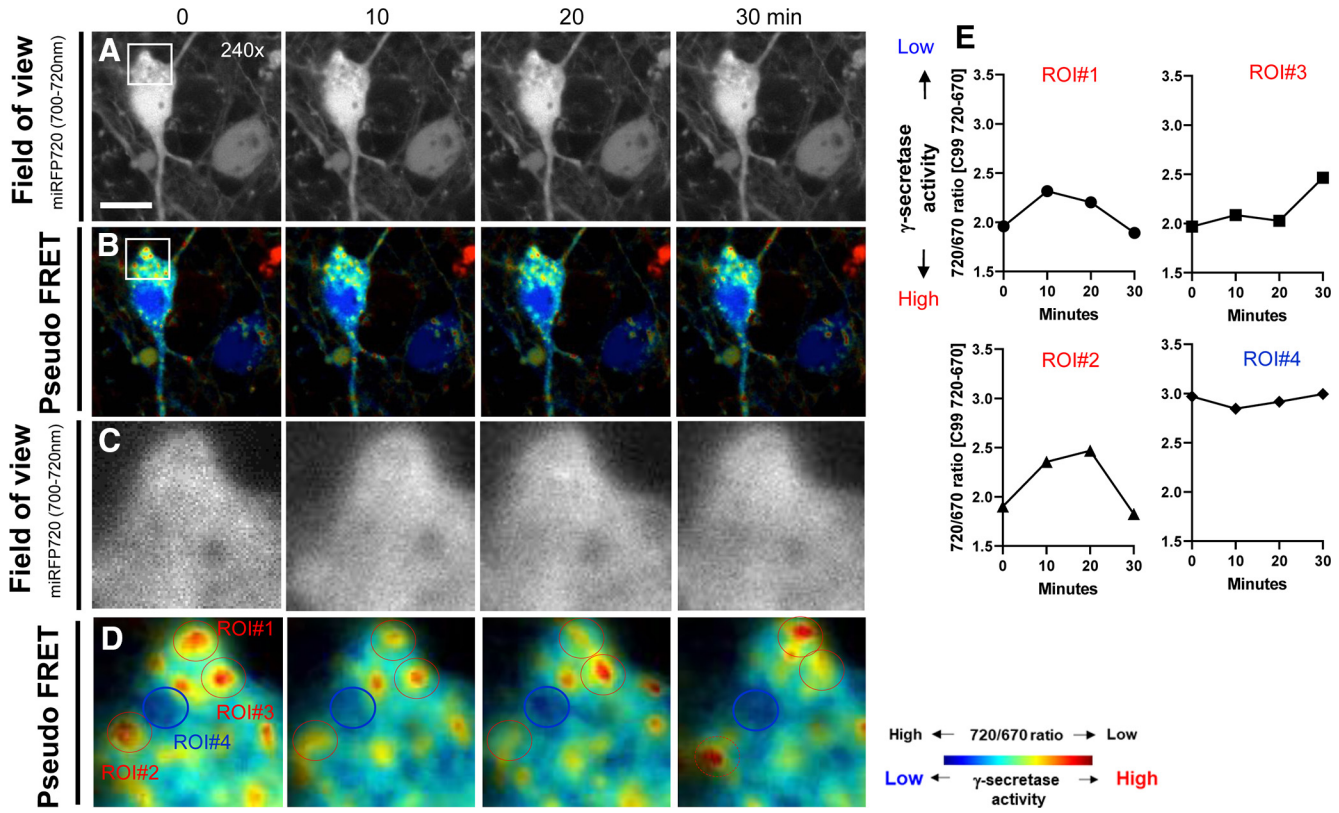

Figure 3. Longitudinal monitoring of the C99 720-670 biosensor processing by γ-secretase with subcellular resolution. The emission of miRFP670 (donor) and 720 (acceptor) in primary neurons expressing the C99 720-670 biosensor was monitored every 10 min for 30 min. miRFP720 emission (field of view; ***A***) and pseudo-colored miRFP720 over 670 emission ratios (pseudo-colored FRET; ***B***) from every 10-min imaging points. Scale bar: 10 μm. Higher magnification images corresponding to the squared area in Figure 2*A*,*B* (***C***, ***D***). Quantitative analysis of 720/670 ratios in four different ROIs corresponding to Figure 2*D* (***E***).

captures the N-terminal epitope of human C99 (1–16 aa), and thus labels both the C99 720-670 biosensor and the intracellular Aβ derived from the biosensor (Fig. 4*A*). We verified that 6E10 emission signal is not positively correlated with the expression level of C99 720-670 biosensor (i.e., miRFP720 emission; Fig. 4*B*). More importantly, γ-secretase inhibitor (1 μM DAPT) treatment significantly decreased 6E10 over C99 720-670 emission ratios (Fig. 4*C*). These results demonstrate the successful staining of intracellular Aβ by the 6E10 antibody, enabling us to interpret the cell compartment(s) with increased 6E10 A488/C99 720-670 expression ratios as sites where intracellular Aβ is significantly accumulated.

We examined whether the cell compartments where γ-secretase primarily processes the C99 720-670 biosensor overlap with those in which intracellular Aβ is accumulated. As such, the C99 720-670 expressing neurons were stained with the 6E10 antibody, followed by staining with an Alexa Fluor 488-conjugated secondary antibody. Then, the neurons were sequentially excited by 488 nm and 640 nm lasers, and Alexa Fluor 488, miRFP670, and miRFP720 emission were detected to measure their emission intensity (Fig. 4*D*–*F*). To "visualize" the compartments where γ-secretase cleaves the C99 720-670 biosensor, miRFP720 emission was divided by that of miRFP670. The area with a lower 720/670 ratio (i.e., more processing) was color-coded in red while the higher ratio was blue (Fig. 4*G*). Next, 6E10-A488 emission was divided by the miRFP720 emission indicative of the C99 720-670 biosensor expression level. The areas with higher (i.e., more intracellular Aβ) and lower 6E10-A488/720 ratios were color-coded in red and blue, respectively (Fig. 4*H*). We found that the subcellular compartments where γ-secretase actively processes the C99 720-670 biosensor strikingly overlap with those containing intracellular Aβ (Fig. 4*G*,*H*). These results suggest that intracellular Aβ is accumulated in the same areas where γ-secretase processes the C99 720-670 biosensor.

To further validate the accumulation of Aβ in late endosomes and lysosomes, neurons expressing the C99 720-670 biosensor were stained with 6E10 and the antibodies against endo-lysosomal marker proteins. As a result, we uncovered that the subcellular loci with increased 6E10/720 ratios (i.e., enrichment of intracellular Aβ) are also positive with the LAMP1 (Fig. 5*A*), moderately overlaps with Rab7 (Fig. 5*B*), and rarely with Rab5 (Fig. 5*C*). Taken together, these results strongly suggest that γ-secretase primarily processes the C99 720-670 biosensor in late endosomes and lysosomes of neurons, resulting in local accumulation of intracellular Aβ in the same subcellular areas.

The pH of late endosomes and lysosomes is linked to cellular γ-secretase activity

We have previously uncovered that γ-secretase activity is heterogeneously regulated among neurons (Maesako et al., 2020). Therefore, we examined whether the pH of endo-lysosomal pathway is functionally linked to cellular γ-secretase activity in live neurons. As such, we incubated neurons expressing the C99 720-670 biosensor with LysoTracker Green and examined whether there is a correlation between 720/670 ratios (γ-secretase activity) and LysoTracker Green fluorescence intensity on a cell-by-cell basis. Interestingly, we found a statistically significant negative correlation between 720/670 ratios and LysoTracker

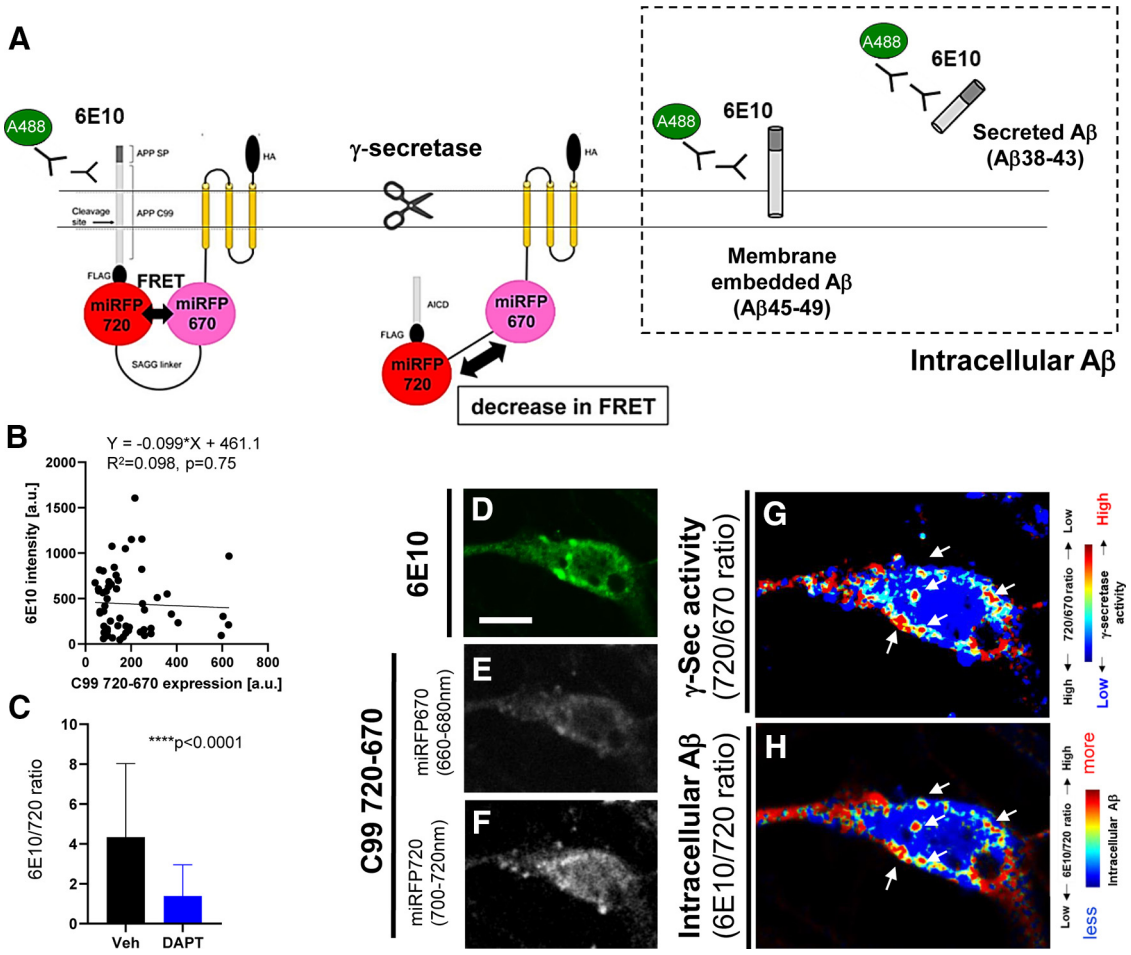

Figure 4. Visualization of intracellular Aβ derived from the C99 720-670 biosensor in neurons. ***A***, A schematic representation of the immunostaining approach distinguishing Aβ from the C99 720-670 biosensors. ***B***, No correlation between 6E10 emission intensity and C99 720-670 biosensor expression levels (i.e., miRFP720 emission); $n = 58$ neurons, $Y = -0.099\times + 461.1$, $R^2 = 0.098$, n.s. $p = 0.75$ (***C***) 6E10 over miRFP720 emission ratios are significantly decreased by the treatment with 1 μM DAPT, a potent γ-secretase inhibitor; $n = 50$ neurons, Mann–Whitney *U* test, $^{****}p < 0.0001$. Primary neurons expressing the C99 720-670 biosensor were immunostained with the 6E10 antibody, followed by an Alexa Fluor 488-conjugated secondary antibody. Representative images of the 6E10 intensity (***D***), miRFP670 (***E***), and miRFP720 (***F***). Pseudo-colored images corresponding the 720/670 ratios (i.e., lower ratio = more γ-secretase activity: highlighted by red; ***G***) and 6E10/720 ratios (i.e., higher ratio = more intracellular Aβ, which is highlighted by red; ***H***). Scale bar: 10 μm.

Green intensity (Fig. 6*A*,*B*). To verify this finding by a more quantitative approach, primary neurons expressing the C99 720-670 biosensor were incubated with LysoSensor Yellow/Blue DND-160. Strikingly, the Yellow/Blue ratios were negatively correlated with 720/670 ratios (Fig. 6*C*,*D*). Furthermore, we used a pH sensitive dye-conjugated Dextran (pHrodo Green Dextran, 10,000 MW) which emits fluorescence after being endocytosed and reaching acidic compartments. We found pHrodo Green Dextran intensity also negatively correlates with 720/670 ratios (Fig. 6*E*,*F*). To determine whether the lower pHrodo Dextran intensity in the neurons with lower γ-secretase activity is because of insufficient endocytosis, we performed time-lapse live-cell imaging in which pHrodo Dextran intensity was measured 10 and 20 min after incubation in individual neurons. The ratio of intensity at 20 over that at 10 min (i.e., $\Delta F/F$) was calculated on a cell-by-cell basis and was interpreted as the efficiency of endocytosis in each cell. We found that there was no correlation between $\Delta F/F$ and γ-secretase activity (Fig. 6*G*), suggesting that the rate of endocytosis was similar in neurons with different γ-secretase activity. Taken together, these results demonstrate functional correlation between the endo-lysosomes pH and cellular γ-secretase activity.

Discussion

γ-Secretase plays a pivotal role in physiological and pathologic conditions in neurons. However, precisely where within the neuron γ-secretase processes its substrate(s) (e.g., APP C99) has not been fully addressed. To directly visualize the γ-secretase activity and its derived products in intact neurons with subcellular resolution, we employed new multiplexed FRET imaging by using our recently developed C99 720-670 biosensor (Houser et al., 2020). Here, we demonstrate that γ-secretase primarily cleaves the C99 720-670 biosensor in acidic compartments in mouse cortex primary neurons (Figs. 1, 2). One can assume that decreased 720/670 ratios, which we interpreted as the activation of γ-secretase, might be because of the low pH in acidic compartments, simply affecting the fluorescent properties of the C99 720-670 biosensor. However, the brightness of miRFP670 is comparable to that of miRFP720 in a pH 4.5–5.0 range (i.e., lysosomes pH; Shcherbakova et al., 2018). More importantly, we observed dynamic fluctuations in 720/670 ratios (Fig. 3). Furthermore, we showed that Aβ is significantly concentrated in the same subcellular location (Figs. 4, 5). Lastly, we identified that the higher endo-lysosomal pH is associated with decreased cellular activity of γ-secretase (Fig. 6). Altogether, our findings

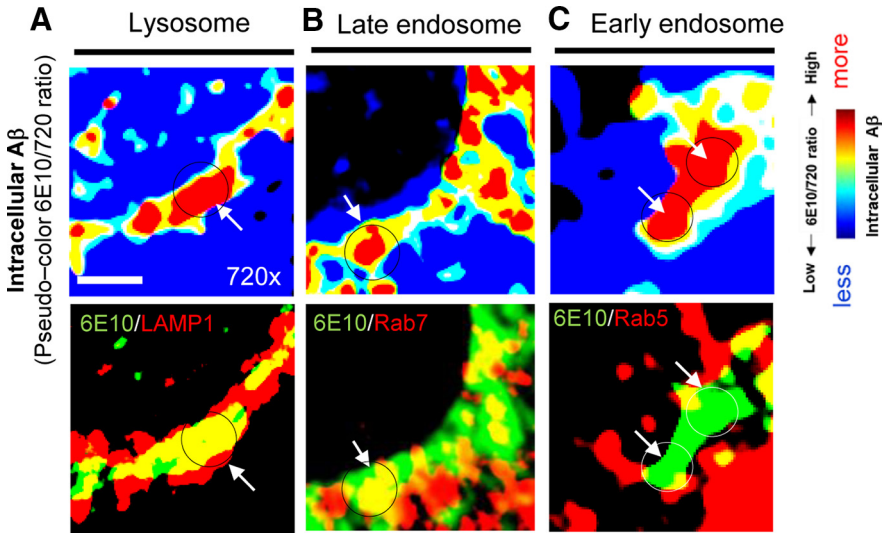

Figure 5. Colocalization analysis of intracellular Aβ and endo-lysosomal markers. ***A***, Higher magnification pseudo-colored images corresponding the 6E10/720 ratios (i.e., higher ratio = more intracellular Aβ, which is highlighted by red) and LAMP1 (a lysosome marker), (***B***) Rab7 (late endosome), or (***C***) Rab5 (early endosome), indicating predominant localization of intracellular Aβ in lysosomes. Scale bar: 2 μm.

strongly suggest that C99 is predominantly processed by γ-secretase and Aβ is accumulated within acidic compartments such as lysosomes and late endosomes in living neurons.

Numerous mutations have been discovered in the genes encoding the catalytic subunit of γ-secretase (PSEN1 and PSEN2) and a γ-secretase substrate (APP; https://www.alzforum.org/mutations). While over 150 different transmembrane proteins have been reported as substrates of γ-secretase (Haapasalo and Kovacs, 2011; Güner and Lichtenthaler, 2020), mutations resulting in early onset of the disease are identified only in the APP gene, specifically in and around the region encoding Aβ. These facts strongly support the hypothesis that APP processing by γ-secretase is mechanistically essential in the development and progression of FAD. Although changes in the γ-secretase activity by FAD mutations could result in different expressions of C99, Aβ peptides (intracellular and extracellular) and AICD, "extracellular" Aβ, Aβ42 in particular, has gained prominence as a pathogenic candidate. This could be because Aβ42 is the main component of neuritic plaques (Iwatsubo et al., 1994). It also readily forms Aβ oligomers, a species that has been shown to disrupt synaptic functions, decrease the number synapses and cause memory impairment in animal models (Lesné et al., 2006; Shankar et al., 2008; Koffie et al., 2009). Various studies demonstrate that FAD mutations drive variable effect on the ε cleavage of C99 (i.e., AICD production) but a consistent reduction carboxypeptidase-like activity of γ-secretase, resulting in an increase in Aβ42 levels compared with shorter Aβ species such as Aβ40 and Aβ38 (Quintero-Monzon et al., 2011; Chávez-Gutiérrez et al., 2012; Fernandez et al., 2014; Szaruga et al., 2015). Nevertheless, recent comprehensive studies analyzing a broad range of FAD mutations uncovered several FAD mutations that do not elevate the Aβ42/Aβ40 ratio (Sun et al., 2017; Devkota et al., 2021), requiring reconsideration of pathogenic mechanism(s) leading to FAD.

Technical challenges in detecting "intracellular" Aβ could also contribute to the predominant investigation of extracellular Aβ. Early studies employing biochemical approaches enabled the detection and quantification of extracellular Aβ (for review, see Masters and Selkoe, 2012). More importantly, imaging agents that specifically bind to the β-sheet structure of Aβ fibril have been engineered (Klunk et al., 2002) to visualize extracellularly accumulated Aβ in postmortem tissues and the intact brain of animal models (Meyer-Luehmann et al., 2008) and AD patients (Klunk et al., 2004). On the other hand, the visualization of intracellular Aβ has remained challenging since the antibodies against Aβ capture both intracellular Aβ and full-length APP and/or C99, causing difficulty in ensuring the existence of intracellular Aβ and elucidating its cellular consequences. Although the 6E10 antibody used in this study recognizes both the C99 720-670 biosensor and intracellular Aβ, we normalized the Alexa Fluor 488-labeled 6E10 fluorescent signal to that of the C99 720-670 biosensor, enabling us to distinguish intracellular Aβ signal (only A488 positive) from C99 (A488 and 720-positive; Fig. 4). More importantly, we were able not only to distinguish Aβ and C99 but also to directly visualize the overlap between intracellular Aβ and the activity of endogenous γ-secretase in specific compartments (Fig. 4). The unique spectral property of NIR fluorescent proteins such as miRFP670 and miRFP720 permits the use of two different colors in the visible spectrum range; this ability allows monitoring another biological event in the same cell (for example, C99 720-670 and 6E10-Alexa Fluor 488 are to separate C99 and intracellular Aβ, galectin-Cy3: lysosome membrane integrity, etc.). Therefore, this new immunostaining approach will permit examination of the exact consequences of intracellular Aβ.

Of note, accumulating evidence also highlights the essential role of C99 in endo-lysosomal compartments. For instance, it is reported using APP transgenic mice and the direct expression of C99 with an AAV that C99 accumulation results in disrupted lysosomal proteolysis (Lauritzen et al., 2016). An endo-lysosomal abnormality that includes enlargement of early endosomes is also observed in the Down syndrome models expressing three copies of APP genes, rescued by pharmacological and genetic inhibition of BACE1 but enhanced by γ-secretase inhibition (Jiang et al., 2010, 2016). Furthermore, recent iPSCs cellular models with FAD mutations illustrate a causal relationship between C99 accumulation and endo-lysosomal dysfunctions (Hung and Livesey, 2018; Kwart et al., 2019). Taken together, C99 could be responsible for the alkalization of the endo-lysosomal pathway we uncovered in the neurons with lower γ-secretase activity (Fig. 6). C99, the membrane-embedded, and the secreted Aβ are localized on the membrane and in the lumen of late endosomes and lysosomes, respectively. Thus, how each catabolite functions in the essential cellular compartments would be critical for better understanding AD etiology.

Evidence from animal models suggests that Tau pathology is accelerated in the presence of Aβ pathology (Pérez et al., 2005; Hurtado et al., 2010; Saul et al., 2013). However, these two pathologic alterations co-occur with different topological and temporal

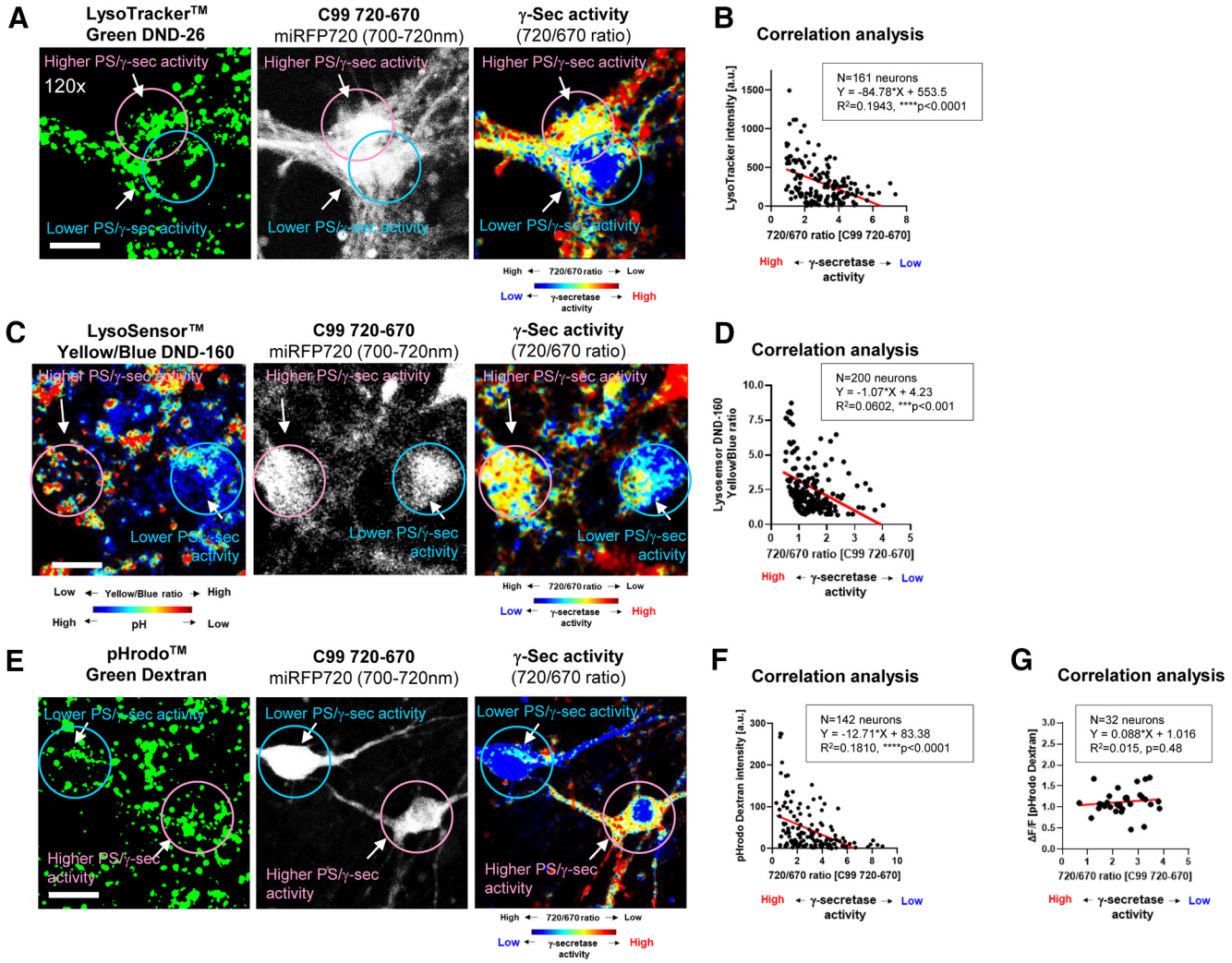

Figure 6. Functional correlation between γ-secretase activity and endo-lysosomal pH. Primary neurons expressing the C99 720-670 biosensor were incubated with pH indicators: LysoTracker Green DND-26, LysoSensor Yellow/Blue DND-160, or pHrodo Green Dextran, 10,000 MW. ***A***, The emission of miRFP670 (donor) and 720 (acceptor) was measured on a cell-by-cell basis in live neurons. Then, LysoTracker Green emission was measured in the same neurons. The LysoTracker Green emission (first panel), the miRFP720 emission represents C99 720-670 biosensor expression (second panel, field of view), and the 720/670 ratios are corresponding to γ-secretase activity (third panel, pseudo-color FRET, red = higher activity). ***B***, The 720/670 ratios are negatively correlated with LysoTracker Green intensity ($n = 161$ neurons, $Y = -84.78\times + 553.5$, $R^2 = 0.1943$, $^{****}p < 0.0001$). Similarly, representative images from the neurons with LysoSensor Yellow/Blue DND-160 (***C***) or pHrodo Green Dextran (***E***), and the negative correlation between the 720/670 ratios and the LysoSensor Yellow/Blue ratios ($n = 200$ neurons, $Y = -1.07\times + 4.23$, $R^2 = 0.0602$, $^{***}p < 0.001$; ***D***) or pHrodo Green Dextran intensity ($n = 142$ neurons, $Y = -12.71\times + 83.38$, $R^2 = 0.1810$, $^{****}p < 0.0001$; ***F***) is shown. ***G***, In the time lapse imaging, pHRodo Green Dextran intensity after 20 min was divided by that at 10 min in individual neurons to calculate ΔF/F, which implicates endocytosis efficiency. There was no correlation between ΔF/F (i.e., endocytosis) and 720/670 ratios (i.e., γ-secretase activity; $n = 32$ neurons, $Y = 0.088\times + 1.016$, $R^2 = 0.015$, $p = 0.48$).

patterns, leading the field to wonder how and where in neurons the two key players in AD, Aβ and Tau, functionally interact with each other. Our current FRET-based study supports earlier biochemical studies showing that Aβ is intracellularly generated (Fig. 1–3) and primarily concentrated (Figs. 4, 5) in late endosomes and/or lysosomes. However, the pH optimum for γ-secretase activity is reported as around 6.3–7.0 (Li et al., 2000; Campbell et al., 2003; Fraering et al., 2004; Fukumori et al., 2006; Quintero-Monzon et al., 2011), which is different from late endosomal and lysosomal pH. On the other hand, γ-secretase has a broad pH range and retains considerable activity at lower pHs. Furthermore, previous studies illustrated that, while PSEN1/γ-secretase is broadly expressed within the entire cells, PSEN2/γ-secretase is predominantly localized in late endosomes and lysosomes (Meckler and Checler, 2016; Sannerud et al., 2016; Watanabe et al., 2021). Therefore, we predict the prominent processing of C99 720-670 biosensor by γ-secretase and the accumulation of Aβ in these compartments could be because the actual expression of functional γ-secretase complexes (i.e., PSEN1 "plus" PSEN2/γ-secretase) is higher in the acidic subcellular loci than other areas. Interestingly, emerging evidence suggests endo-lysosomal pathway is tightly associated with Tau propagation and aggregation (Rauch et al., 2020; Polanco and Götz, 2021; Polanco et al., 2021). If this is the case, late endosomes and/or lysosomes could be where, APP, γ-secretase, and Tau intersect to initiate neurodegeneration.

In conclusion, our novel, high-resolution, multiplexing, live-cell FRET imaging uncovered that γ-secretase processes C99 primarily within low-pH compartments in neurons. This processing is a spatiotemporally dynamic and heterogeneous event. Furthermore, we developed a new immunostaining protocol that enabled the visualization of intracellular Aβ, and found that intracellular Aβ is significantly accumulated in the

same compartments where γ-secretase processes C99. Remaining key questions such as which Aβ species are predominantly accumulated, what is the exact consequence of intracellular Aβ accumulation in acidic compartments, and importantly whether the accumulation of Aβ in these compartments is relevant to AD will be investigated in the future studies.

References

Berezovska O, Ramdya P, Skoch J, Wolfe MS, Bacskai BJ, Hyman BT (2003) Amyloid precursor protein associates with a nicastrin-dependent docking site on the presenilin 1-γ-secretase complex in cells demonstrated by fluorescence lifetime imaging. J Neurosci 23:4560–4566.

Campbell WA, Reed ML, Strahle J, Wolfe MS, Xia W (2003) Presenilin endoproteolysis mediated by an aspartyl protease activity pharmacologically distinct from γ-secretase. J Neurochem 85:1563–1574.

Chávez-Gutiérrez L, Bammens L, Benilova I, Vandersteen A, Benurwar M, Borgers M, Lismont S, Zhou L, Van Cleynenbreugel S, Esselmann H, Wiltfang J, Serneels L, Karran E, Gijsen H, Schymkowitz J, Rousseau F, Broersen K, De Strooper B (2012) The mechanism of γ-secretase dysfunction in familial Alzheimer disease. EMBO J 31:2261–2274.

Cupers P, Bentahir M, Craessaerts K, Orlans I, Vanderstichele H, Saftig P, De Strooper B, Annaert W (2001) The discrepancy between presenilin subcellular localization and gamma-secretase processing of amyloid precursor protein. J Cell Biol 154:731–740.

De Strooper B, Saftig P, Craessaerts K, Vanderstichele H, Guhde G, Annaert W, Von Figura K, Van Leuven F (1998) Deficiency of presenilin-1 inhibits the normal cleavage of amyloid precursor protein. Nature 391:387–390.

Devkota S, Williams TD, Wolfe MS (2021) Familial Alzheimer's disease mutations in amyloid protein precursor alter proteolysis by γ-secretase to increase amyloid β-peptides of ≥45 residues. J Biol Chem 296:100281.

Escamilla-Ayala AA, Sannerud R, Mondin M, Poersch K, Vermeire W, Paparelli L, Berlage C, Koenig M, Chavez-Gutierrez L, Ulbrich MH, Munck S, Mizuno H, Annaert W (2020) Super-resolution microscopy reveals majorly mono- and dimeric presenilin1/γ-secretase at the cell surface. Elife 9:e56679.

Fernandez MA, Klutkowski JA, Freret T, Wolfe MS (2014) Alzheimer presenilin-1 mutations dramatically reduce trimming of long amyloid β-peptides (Aβ) by γ-secretase to increase 42-to-40-residue Aβ. J Biol Chem 289:31043–31052.

Fraering PC, Ye W, Strub JM, Dolios G, LaVoie MJ, Ostaszewski BL, van Dorsselaer A, Wang R, Selkoe DJ, Wolfe MS (2004) Purification and characterization of the human gamma-secretase complex. Biochemistry 43:9774–9789.

Fukumori A, Okochi M, Tagami S, Jiang J, Itoh N, Nakayama T, Yanagida K, Ishizuka-Katsura Y, Morihara T, Kamino K, Tanaka T, Kudo T, Tanii H, Ikuta A, Haass C, Takeda M (2006) Presenilin-dependent gamma-secretase on plasma membrane and endosomes is functionally distinct. Biochemistry 45:4907–4914.

Funamoto S, Morishima-Kawashima M, Tanimura Y, Hirotani N, Saido TC, Ihara Y (2004) Truncated carboxyl-terminal fragments of beta-amyloid precursor protein are processed to amyloid beta-proteins 40 and 42. Biochemistry 43:13532–13540.

Güner G, Lichtenthaler SF (2020) The substrate repertoire of g-secretase/presenilin. Semin Cell Dev Biol 105:27–42.

Haapasalo A, Kovacs DM (2011) The many substrates of presenilin/g-secretase. J Alzheimers Dis 25:3–28.

Haass C, Koo EH, Mellon A, Hung AY, Selkoe DJ (1992) Targeting of cell-surface beta-amyloid precursor protein to lysosomes: alternative processing into amyloid-bearing fragments. Nature 357:500–503.

Houser MCQ, Hou SS, Perrin F, Turchyna Y, Bacskai BJ, Berezovska O, Maesako M (2020) A novel NIR FRET biosensor for reporting PS/γ-secretase activity in live cells. Sensors 20:5980.

Hung COY, Livesey FJ (2018) Altered gamma-secretase processing of APP disrupts lysosome and autophagosome function in monogenic Alzheimer's disease. Cell Rep 25:3647–3660.e2.

Hurtado DE, Molina-Porcel L, Iba M, Aboagye AK, Paul SM, Trojanowski JQ, Lee VM (2010) Aβ accelerates the spatiotemporal progression of tau pathology and augments tau amyloidosis in an Alzheimer mouse model. Am J Pathol 177:1977–1988.

Iwatsubo T, Odaka A, Suzuki N, Mizusawa H, Nukina N, Ihara Y (1994) Visualization of A β 42(43) and A β 40 in senile plaques with end-specific A β monoclonals: evidence that an initially deposited species is A β 42(43). Neuron 13:45–53.

Jiang Y, Mullaney KA, Peterhoff CM, Che S, Schmidt SD, Boyer-Boiteau A, Ginsberg SD, Cataldo AM, Mathews PM, Nixon RA (2010) Alzheimer's-related endosome dysfunction in Down syndrome is Abeta-independent but requires APP and is reversed by BACE-1 inhibition. Proc Natl Acad Sci USA 107:1630–1635.

Jiang Y, Rigoglioso A, Peterhoff CM, Pawlik M, Sato Y, Bleiwas C, Stavrides P, Smiley JF, Ginsberg SD, Mathews PM, Levy E, Nixon RA (2016) Partial BACE1 reduction in a down syndrome mouse model blocks Alzheimer-related endosomal anomalies and cholinergic neurodegeneration: role of APP-CTF. Neurobiol Aging 39:90–98.

Klunk WE, Bacskai BJ, Mathis CA, Kajdasz ST, McLellan ME, Frosch MP, Debnath ML, Holt DP, Wang Y, Hyman BT (2002) Imaging Aβ plaques in living transgenic mice with multiphoton microscopy and methoxy-X04, a systemically administered Congo red derivative. J Neuropathol Exp Neurol 61:797–805.

Klunk WE, Engler H, Nordberg A, Wang Y, Blomqvist G, Holt DP, Bergström M, Savitcheva I, Huang GF, Estrada S, Ausén B, Debnath ML, Barletta J, Price JC, Sandell J, Lopresti BJ, Wall A, Koivisto P, Antoni G, Mathis CA, et al. (2004) Imaging brain amyloid in Alzheimer's disease with Pittsburgh Compound-B. Ann Neurol 55:306–319.

Koffie RM, Meyer-Luehmann M, Hashimoto T, Adams KW, Mielke ML, Garcia-Alloza M, Micheva KD, Smith SJ, Kim ML, Lee VMY, Hyman BT, Spires-Jones TL (2009) Oligomeric amyloid β associates with postsynaptic densities and correlates with excitatory synapse loss near senile plaques. Proc Natl Acad Sci USA 106:4012–4017.

Koo EH, Squazzo SL (1994) Evidence that production and release of amyloid beta-protein involves the endocytic pathway. J Biol Chem 269:17386–17389.

Koo EH, Squazzo SL, Selkoe DJ, Koo CH (1996) Trafficking of cell-surface amyloid beta-protein precursor. I. Secretion, endocytosis and recycling as detected by labeled monoclonal antibody. J Cell Sci 109:991–998.

Kwart D, Gregg A, Scheckel C, Murphy EA, Paquet D, Duffield M, Fak J, Olsen O, Darnell RB, Tessier-Lavigne M (2019) A large panel of isogenic APP and PSEN1 mutant human iPSC neurons reveals shared endosomal abnormalities mediated by APP β-CTFs, not Aβ. Neuron 104:1022.

Lai MT, Chen E, Crouthamel MC, DiMuzio-Mower J, Xu M, Huang Q, Price E, Register RB, Shi XP, Donoviel DB, Bernstein A, Hazuda D, Gardell SJ, Li YM (2003) Presenilin-1 and presenilin-2 exhibit distinct yet overlapping γ-secretase activities. J Biol Chem 278:22475–22481.

Lauritzen I, Pardossi-Piquard R, Bourgeois A, Pagnotta S, Biferi MG, Barkats M, Lacor P, Klein W, Bauer C, Checler F (2016) Intraneuronal aggregation of the β-CTF fragment of APP (C99) induces Aβ-independent lysosomal-autophagic pathology. Acta Neuropathol 132:257–276.

Lauritzen I, Pardossi-Piquard R, Bourgeois A, Bécot A, Checler F (2019) Does intraneuronal accumulation of carboxyl-terminal fragments of the amyloid precursor protein trigger early neurotoxicity in Alzheimer's disease? Curr Alzheimer Res 16:453–457.

Lesné S, Koh MT, Kotilinek L, Kayed R, Glabe CG, Yang A, Gallagher M, Ashe KH (2006) A specific amyloid-β protein assembly in the brain impairs memory. Nature 440:352–357.

Levy-Lahad E, Wasco W, Poorkaj P, Romano DM, Oshima J, Pettingell WH, Yu CE, Jondro PD, Schmidt SD, Wang K (1995) Candidate gene for the chromosome 1 familial Alzheimer's disease locus. Science 269:973–977.

Li YM, Lai MT, Xu M, Huang Q, DiMuzio-Mower J, Sardana MK, Shi XP, Yin KC, Shafer JA, Gardell SJ (2000) Presenilin 1 is linked with gamma-secretase activity in the detergent solubilized state. Proc Natl Acad Sci USA 97:6138–6143.

Maesako M, Horlacher J, Zoltowska KM, Kastanenka KV, Kara E, Svirsky S, Keller LJ, Li X, Hyman BT, Bacskai BJ, Berezovska O (2017) Pathogenic PS1 phosphorylation at Ser367. Elife 6:e19720.

Maesako M, Sekula NM, Aristarkhova A, Feschenko P, Anderson LC, Berezovska O (2020) Visualization of PS/γ-secretase activity in living cells. iScience 23:101139.

Masters CL, Selkoe DJ (2012) Biochemistry of amyloid β-protein and amyloid deposits in Alzheimer disease. Cold Spring Harb Perspect Med 2: a006262.

Meckler X, Checler F (2016) Presenilin 1 and presenilin 2 target γ-secretase complexes to distinct cellular compartments. J Biol Chem 291:12821–12837.

Meyer-Luehmann M, Spires-Jones TL, Prada C, Garcia-Alloza M, de Calignon A, Rozkalne A, Koenigsknecht-Talboo J, Holtzman DM, Bacskai BJ, Hyman BT (2008) Rapid appearance and local toxicity of amyloid-beta plaques in a mouse model of Alzheimer's disease. Nature 451:720–724.

Pardossi-Piquard R, Checler F (2012) The physiology of the β-amyloid precursor protein intracellular domain AICD. J Neurochem 120 [Suppl 1]:109–124.

Pasternak SH, Bagshaw RD, Guiral M, Zhang S, Ackerley CA, Pak BJ, Callahan JW, Mahuran DJ (2003) Presenilin-1, nicastrin, amyloid precursor protein, and gamma-secretase activity are co-localized in the lysosomal membrane. J Biol Chem 278:26687–26694.

Pérez M, Ribe E, Rubio A, Lim F, Morán MA, Ramos PG, Ferrer I, Isla MT, Avila J (2005) Characterization of a double (amyloid precursor protein-tau) transgenic: tau phosphorylation and aggregation. Neuroscience 130:339–347.

Placanica L, Tarassishin L, Yang G, Peethumnongsin E, Kim SH, Zheng H, Sisodia SS, Li YM (2009) Pen2 and presenilin-1 modulate the dynamic equilibrium of presenilin-1 and presenilin-2 gamma-secretase complexes. J Biol Chem 284:2967–2977.

Polanco JC, Götz J (2021) Exosomal and vesicle-free tau seeds-propagation and convergence in endolysosomal permeabilization. FEBS J. Advance online publication. Retrieved June 6, 2021. doi: 10.1111/febs.16055.

Polanco JC, Hand GR, Briner A, Li C, Götz J (2021) Exosomes induce endolysosomal permeabilization as a gateway by which exosomal tau seeds escape into the cytosol. Acta Neuropathol 141:235–256.

Qi-Takahara Y, Morishima-Kawashima M, Tanimura Y, Dolios G, Hirotani N, Horikoshi Y, Kametani F, Maeda M, Saido TC, Wang R, Ihara Y (2005) Longer forms of amyloid beta protein: implications for the mechanism of intramembrane cleavage by gamma-secretase. J Neurosci 25:436–445.

Quintero-Monzon O, Martin MM, Fernandez MA, Cappello CA, Krzysiak AJ, Osenkowski P, Wolfe MS (2011) Dissociation between the processivity and total activity of γ-secretase: implications for the mechanism of Alzheimer's disease-causing presenilin mutations. Biochemistry 50:9023–9035.

Rauch JN, Luna G, Guzman E, Audouard M, Challis C, Sibih YE, Leshuk C, Hernandez I, Wegmann S, Hyman BT, Gradinaru V, Kampmann M, Kosik KS (2020) LRP1 is a master regulator of tau uptake and spread. Nature 580:381–385.

Sannerud R, Esselens C, Ejsmont P, Mattera R, Rochin L, Tharkeshwar AK, De Baets G, De Wever V, Habets R, Baert V, Vermeire W, Michiels C, Groot AJ, Wouters R, Dillen K, Vints K, Baatsen P, Munck S, Derua R, Waelkens E, et al. (2016) Restricted location of PSEN2/γ-secretase determines substrate specificity and generates an intracellular Aβ pool. Cell 166:193–208.

Saul A, Sprenger F, Bayer TA, Wirths O (2013) Accelerated tau pathology with synaptic and neuronal loss in a novel triple transgenic mouse model of Alzheimer's disease. Neurobiol Aging 34:2564–2573.

Schrader-Fischer G, Paganetti PA (1996) Effect of alkalizing agents on the processing of the β-amyloid precursor protein. Brain Res 716:91–100.

Selkoe DJ, Hardy J (2016) The amyloid hypothesis of Alzheimer's disease at 25 years. EMBO Mol Med 8:595–608.

Sevigny J, Chiao P, Bussière T, Weinreb PH, Williams L, Maier M, Dunstan R, Salloway S, Chen T, Ling Y, O'Gorman J, Qian F, Arastu M, Li M, Chollate S, Brennan MS, Quintero-Monzon O, Scannevin RH, Arnold HM, Engber T, et al. (2016) The antibody aducanumab reduces Aβ plaques in Alzheimer's disease. Nature 537:50–56.

Shankar GM, Li S, Mehta TH, Garcia-Munoz A, Shepardson NE, Smith I, Brett FM, Farrell MA, Rowan MJ, Lemere CA, Regan CM, Walsh DM, Sabatini BL, Selkoe DJ (2008) Amyloid-β-protein dimers isolated directly from Alzheimer's brains impair synaptic plasticity and memory. Nat Med 14:837–842.

Shcherbakova DM, Baloban M, Emelyanov AV, Brenowitz M, Guo P, Verkhusha VV (2016) Bright monomeric near-infrared fluorescent proteins as tags and biosensors for multiscale imaging. Nat Commun 7:12405.

Shcherbakova DM, Cox Cammer N, Huisman TM, Verkhusha VV, Hodgson L (2018) Direct multiplex imaging and optogenetics of Rho GTPases enabled by near-infrared FRET. Nat Chem Biol 14:591–600.

Sherrington R, Rogaev EI, Liang Y, Rogaeva EA, Levesque G, Ikeda M, Chi H, Lin C, Li G, Holman K, Tsuda T, Mar L, Foncin JF, Bruni AC, Montesi MP, Sorbi S, Rainero I, Pinessi L, Nee L, Chumakov I, et al. (1995) Cloning of a gene bearing missense mutations in early-onset familial Alzheimer's disease. Nature 375:754–760.

Sun L, Zhou R, Yang G, Shi Y (2017) Analysis of 138 pathogenic mutations in presenilin-1 on the in vitro production of Aβ42 and Aβ40 peptides by γ-secretase. Proc Natl Acad Sci USA 114:E476–E485.

Szaruga M, Veugelen S, Benurwar M, Lismont S, Sepulveda-Falla D, Lleo A, Ryan NS, Lashley T, Fox NC, Murayama S, Gijsen H, De Strooper B, Chávez-Gutiérrez L (2015) Qualitative changes in human γ-secretase underlie familial Alzheimer's disease. J Exp Med 212:2003–2013.

Takami M, Nagashima Y, Sano Y, Ishihara S, Morishima-Kawashima M, Funamoto S, Ihara Y (2009) Gamma-secretase: successive tripeptide and tetrapeptide release from the transmembrane domain of beta-carboxyl terminal fragment. J Neurosci 29:13042–13052.

Vassar R, Bennett BD, Babu-Khan S, Kahn S, Mendiaz EA, Denis P, Teplow DB, Ross S, Amarante P, Loeloff R, Luo Y, Fisher S, Fuller J, Edenson S, Lile J, Jarosinski MA, Biere AL, Curran E, Burgess T, Louis JC, et al. (1999) Beta-secretase cleavage of Alzheimer's amyloid precursor protein by the transmembrane aspartic protease BACE. Science 286:735–741.

Watanabe H, Imaizumi K, Cai T, Zhou Z, Tomita T, Okano H (2021) Flexible and accurate substrate processing with distinct presenilin/γ-secretases in human cortical neurons. eNeuro 8:ENEURO.0500-20.2021.

Wolfe MS, Xia W, Ostaszewski BL, Diehl TS, Kimberly WT, Selkoe DJ (1999) Two transmembrane aspartates in presenilin-1 required for presenilin endoproteolysis and gamma-secretase activity. Nature 398:513–517.